RSC Advances

COMMUNICATION

View Article Online
View Journal | View Issue

Cite this: *RSC Adv.*, 2015, **5**, 30522

Received 10th March 2015
Accepted 24th March 2015

DOI: 10.1039/c5ra04015a

www.rsc.org/advances

A BODIPY-based fluorescent probe for the differential recognition of Hg(II) and Au(III) ions†

Ceren Cantürk, Muhammed Üçüncü and Mustafa Emrullahoğlu*

Open Access Article. Published on 24 March 2015. Downloaded on 6/7/2026 7:29:38 AM.
This article is licensed under a Creative Commons Attribution 3.0 Unported Licence.

We describe the design, synthesis and spectral behaviour of a fluorescent molecular sensor able to recognize Hg^{2+} and Au^{3+} ions *via* different emission modes. The molecular sensor is constructed on a single BODIPY dye appended with a semithio-carbazone functionality as a recognition motif.

In recent years, research on the development of molecular sensors for analysing diverse biologically and environmentally important analyte species has increased.[1] While the vast majority of sensors addressed in such literature are designed to recognize a specific target, less common are sensors capable of differentiating multiple targets. Differential detection of multiple analyte species can be achieved best by recognizing each species through a different signal output (*i.e.*, emission wavelength).[2] Incorporating multiple binding motifs onto a single signal-transducing molecule (chromophore/fluorophore) and, as an alternative, combining different transducing molecules have both appeared as efficient routes for sensors with multiple output modes.[3]

Despite recent advances in the field, it remains a challenge to differentiate metal species with similar chemical natures. For example, the ionic species of gold (Au^{3+}) and mercury (Hg^{2+}) share several similarities in terms of binding properties, since both have strong binding affinities toward sulphur species. When accumulated in the biological system, they thus have great potential to interact with sulphur-bearing biomolecules such as enzymes, proteins, and DNA. As a result, these metal species can disturb a series of cellular processes that cause toxicity in humans.[3,4] Tracking these metal species in a living environment with the aid of a fluorescent molecular sensor is thus crucial to evaluating their roles in certain biological processes.

In their structure, most molecular sensors devised for mercury ions use sulphur moieties as a recognition motif.[5] As such, it is always possible that gold and mercury species interfere with each other during their analysis, which could primarily explain why molecular sensors able to differentiate these two metal ions are extremely rare.[6] Molecular tools that can differentiate multiple analytes of a similar chemical nature (*e.g.*, gold[7] and mercury[5,8] ions) are therefore clearly in high demand.

Herein, we designed a molecular sensor with a single fluorophore core appended with semithiocarbazone functionality as the metal ion recognition motif. The fluorophore core, based on a BODIPY dye,[9] is designed to be inactive (*i.e.*, non-emissive) in its initial state yet expected to become active in response to the metal species (Scheme 1). The differential detection of Hg^{2+} and Au^{3+} relies on different modulation mechanisms and can be realized with two distinct fluorescence changes, based on either an Hg^{2+}-ligand coordination event or a gold-mediated chemical transformation.

The title compound, **BOD-ZN**, was prepared (40% overall) by the synthetic route outlined in Scheme 1 and, its structure was unambiguously confirmed by ^{1}H-NMR, ^{13}C-NMR, and HRMS spectroscopy.[10]

The sensing behaviour of **BOD-ZN** toward the addition of a range of metal ion species was studied by UV/Vis and fluorescence spectroscopy. As shown in Fig. 1a, the UV/Vis spectrum of free **BOD-ZN** (phosphate buffer/ethanol 1 : 4, pH 7.0) displays a maximum absorption band at 533 nm, which belongs to the

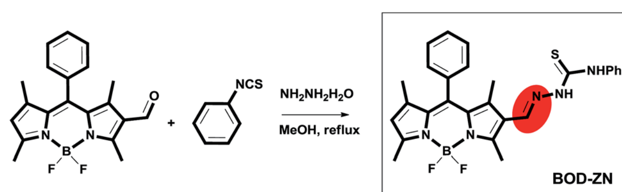

Scheme 1 Synthesis of BOD-ZN.

Department of Chemistry, Faculty of Science, İzmir Institute of Technology, Urla, 35430, Izmir, Turkey. E-mail: mustafaemrullahoglu@iyte.edu.tr

† Electronic supplementary information (ESI) available: Absorbance, fluorescence and characterization data and all experimental procedures. See DOI: 10.1039/c5ra04015a

 This journal is © The Royal Society of Chemistry 2015

Open Access Article. Published on 24 March 2015. Downloaded on 6/7/2026 7:29:38 AM. This article is licensed under a Creative Commons Attribution 3.0 Unported Licence.

BODIPY chromophore. The fluorescence spectrum of **BOD-ZN** collected upon excitation at 460 nm exhibits a very weak emission band at 601 nm. Reasonably, **BOD-ZN** was nearly non-emissive, since the molecular structure of the probe bears a C=N functionality that diminishes the emission of the BODIPY core caused by a non-radiative deactivation process involving the rapid isomerization of the C=N group.

Our investigation began with the evaluation of the optical behaviour of **BOD-ZN** in response to the addition of Au^{3+} ions (*e.g.*, $AuCl_3$). The addition of Au^{3+} (1 equiv.) to **BOD-ZN** prompted the appearance of a new emission band at 512 nm that was assigned to the formation of a new BODIPY derivative (Fig. 1b). The appearance of this new band was accompanied with a distinct change in the solution's emission colour; the red-emitting probe solution became distinctly green, as was clearly visible to the naked eye (Fig. S19, ESI†).

The compound displaying such green emission was isolated and further characterized as **BOD-AL**, the hydrolysis product of **BOD-ZN** (Scheme 2). Evidently, the recognition of Au^{3+} was based on an Au^{3+}-mediated hydrolysis reaction that resulted in the formation of a highly emissive BODIPY derivative (**BOD-AL**).

A systematic titration of **BOD-ZN** with Au^{3+} reveals that emission band intensity increases linearly with the increase in concentration of Au^{3+} in the range of 0.1–100 μM (Fig. S6, ESI†). At the same time, the kinetic study showed that the spectral response toward the addition of Au^{3+} was rapid (<1 min) and

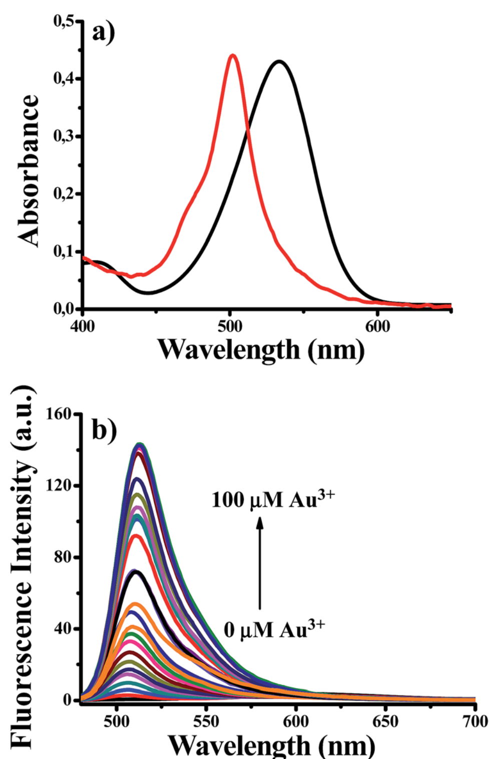

Fig. 1 (a) Absorbance spectra of BOD-ZN (10 μM) in the absence (black line) and presence (red line) of 10 equiv. (100 μM) of Au^{3+}; (b) fluorescence titration spectra of BOD-ZN (10 μM) + Au^{3+} (0.1 to 100 μM, 0.01 to 10 equiv.) in 0.1 M phosphate buffer/EtOH (pH 7.0, v/v, 1 : 4) (25 °C, λ_{ex} = 460 nm).

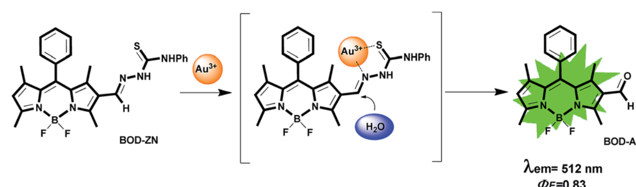

Scheme 2 Hydrolysis mechanism of BOD-ZN in the presence of Au^{3+} ions.

that the emission intensity plateaued within 20 min. Due to the addition of 10 equiv. of Au^{3+}, which thereby enhanced intensity by over 200-fold. Moreover, the minimum amount of Au^{3+} detectable was evaluated to be 128.0 nM based on the signal-to-noise ratio (S/N = 3) (Fig. S2, ESI†).

Having established that the detection of Au^{3+} ions relies on an irreversible chemical reaction, we investigated the selectivity profile of **BOD-ZN** in response to other metal species. The probe proved to be highly specific for Au^{3+} ions, since no change was detected in the spectrum when Au^{+} ions were present. Furthermore, **BOD-ZN** showed no spectral response to other metal ions such as Cu^{2+}, Ag^{+}, Zn^{2+}, Pb^{2+}, Ni^{2+}, Na^{+}, Mg^{2+}, Li^{+}, K^{+}, Pd^{2+}, Co^{2+}, Cd^{2+}, Ca^{2+}, Ba^{2+}, Fe^{3+}, and Cr^{3+}, except for Hg^{2+}.

We recognized the detection of Hg^{2+} with a different emission output. Given the addition of Hg^{2+}, the weakly emissive probe solution immediately (<5 s) turned profoundly yellow, possibly due to the blockage of the C=N isomerization *via* strong coordination to the nitrogen electron pair which prevents the electron transfer process, and thus enhances the fluorescence emission (Scheme 3).

Meanwhile, in the fluorescence spectrum of **BOD-ZN**, a new emission band appeared at 542 nm and increased linearly with the increased concentration of Hg^{2+} above the range of 0.1–100 μM (Fig. 2b). The detection limit of **BOD-ZN** for detecting Hg^{2+} was 160.0 nM.

In sharp contrast to the detection of Au^{3+}, detecting Hg^{2+} ions proceeded reversibly. The reversibility of the binding event between **BOD-ZN** and Hg^{2+} was confirmed by the addition of Na_2S to the solution pre-treated with Hg^{2+}, which sharply decreased the emission intensity. The regeneration of fluorescence was again made possible by introducing Hg^{2+} ions into the solution, and the off-on switching ability of the system with Hg^{2+} proved the reversibility of the process (Fig. S15, ESI†).

At the same time, the binding process of Hg^{2+} to **BOD-ZN** could be clearly followed by the aid of ^{1}H-NMR spectroscopy.

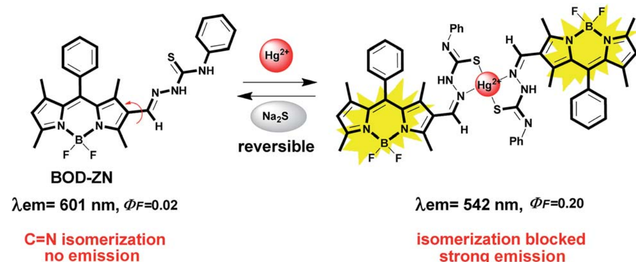

Scheme 3 Reversible binding of Hg^{2+} to BOD-ZN.

Open Access Article. Published on 24 March 2015. Downloaded on 6/7/2026 7:29:38 AM.
This article is licensed under a Creative Commons Attribution 3.0 Unported Licence.

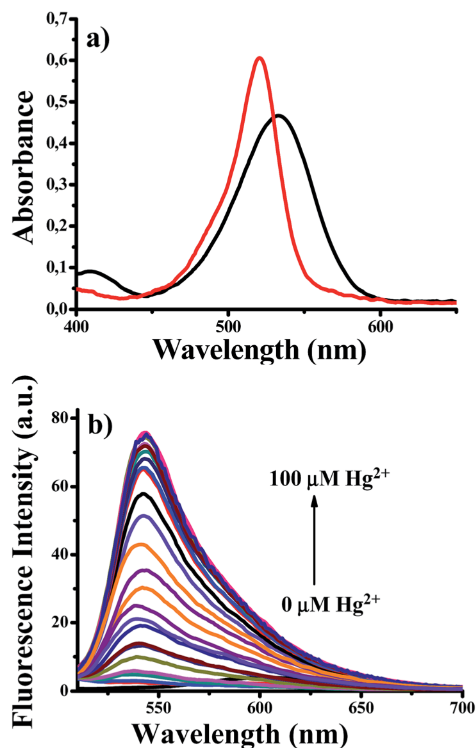

Fig. 2 (a) Absorbance spectra of BOD-ZN (10 μM) in the absence (black line) and presence (red line) of 10 equiv. (100 μM) of Hg^{2+}; (b) fluorescence titration spectra of BOD-ZN (10 μM) + Hg^{2+} (0.1 to 100 μM, 0.01 to 10 equiv.) in 0.1 M phosphate buffer/EtOH (pH 7.0, v/v, 1 : 4) (25 °C, λ_{ex} = 460 nm).

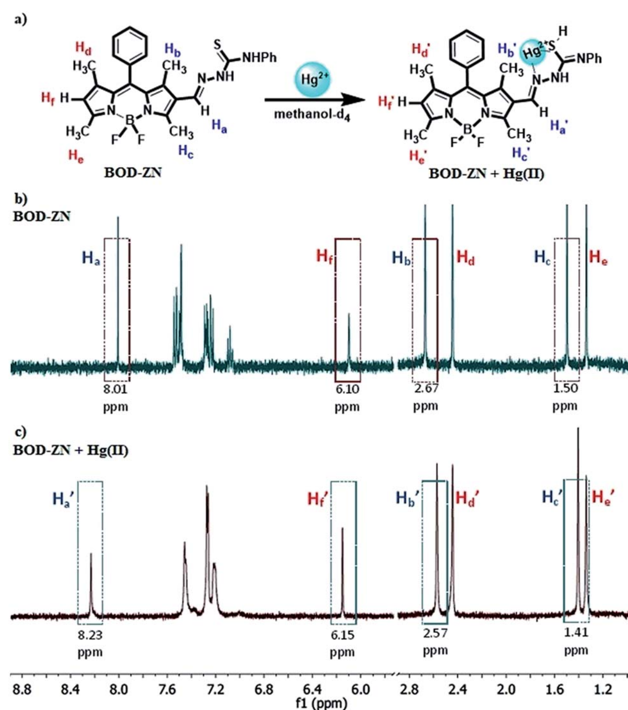

Fig. 3 (a) Proposed coordination mechanism of Hg^{2+} to BOD-ZN; (b) ^{1}H-NMR of BOD-ZN in methanol-d_4; (c) ^{1}H-NMR of BOD-ZN + Hg^{2+} (1 equiv.) in methanol-d_4.

During Hg^{2+} incubation lasting 5 min, we observed pronounced differences in the ^{1}H-NMR spectrum of **BOD-ZN**. For one, the resonance of the H_a proton signal at 8.01 ppm belonging to the hydrogen atom of the aldimine shifted to a higher frequency, while the resonance of the methyl protons (H_b and H_c) in close proximity to the recognition motif shifted to a lower frequency. Furthermore, a reorganization of the phenyl ring proton signals strongly suggests the structural modification in the phenyl thiourea motif (Fig. 3).

The stoichiometry of the sensing event was established by following the Benesi–Hildebrand method and, accordingly, the related binding constant was determined as $4.2 \times 10^4\ M^{-2}$.[11] With HRMS analysis, we also confirmed the binding of Hg^{2+} ions to **BOD-ZN**. HRMS data of the solution (Hg^{2+}/**BOD-ZN**) indicated the formation of an Hg^{2+} ion complex, (m/z = 1204.36841 found; 1204.36354 calc.), with a binding stoichiometry of 1 : 2.[10] Given all of the above, the structure of the binding complex is most likely that shown in Scheme 3.

Having clarified the detection of both metal species, we assessed the interference of other metal ions in the detection of Au^{3+} and Hg^{2+}. Although the spectral response of **BOD-ZN** induced by Au^{3+} ions showed no interference with other metal ions, the detection of Hg^{2+} was disturbed in the presence of Au^{3+} ions. More specifically, in the presence of Au^{3+} and Hg^{2+}, the fluorescence spectrum initially displayed an emission band at 542 nm for the Hg^{2+}/**BOD-ZN** binding complex. However, the band disappeared within 10 min, as a new band appeared at 512 nm, which indicates that Au^{3+} ions also mediate the hydrolysis of the Hg^{2+} binding complex (Fig. S18, ESI†). Notably, the same sensing behaviour was also observed by adding Au^{3+} ions to a solution pre-treated with Hg^{2+}.

Relying on the impressive sensing properties of **BOD-ZN**, we next investigated its capacity for imaging Hg^{2+} and Au^{3+} ions in living cells. As Fig. 4a and a′ show, the images of human lung adenocarcinoma (A549) cells incubated with **BOD-ZN** did not display any fluorescence until the addition of the metal species. However, upon incubation with Au^{3+} or Hg^{2+}, the cells started to emit a distinct fluorescence emission consistent with results obtained in the solution. Based on the nucleus staining experiment using DAPI as the staining dye, we concluded that the probe passes through the cell membrane and detects both

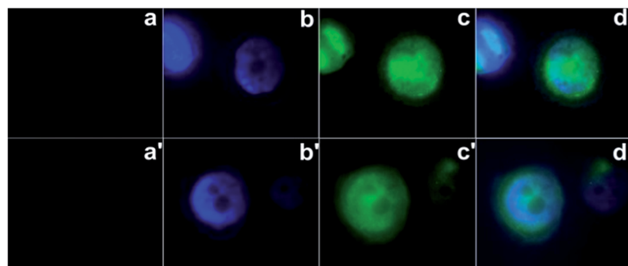

Fig. 4 Fluorescence images of human lung adenocarcinoma cells (A549). (a and a′) Fluorescence image of A549 cells treated with only BOD-ZN (10 μM); (b and b′) fluorescence image of cells treated with DAPI (control); (c and c′) fluorescence image of cells treated with BOD-ZN (10 μM) and Au^{3+} (10 μM) or Hg^{2+} (10 μM) (λ_{ex} = 460 nm); (d and d′) merged images of frames b–c or b′–c′.

Open Access Article. Published on 24 March 2015. Downloaded on 6/7/2026 7:29:38 AM. This article is licensed under a Creative Commons Attribution 3.0 Unported Licence.

metal species from within the cell. This preliminary cell imaging study suggested that **BOD-ZN** can be used efficiently for the *in vitro* imaging of Au^{3+} and Hg^{2+} species in living cells.

Conclusions

To close, we have studied the design, spectral behaviour, and cell-imaging capacity of a unique fluorescent molecular structure that can efficiently differentiate Hg^{2+} and Au^{3+} ions. The differential detection of Hg^{2+} and Au^{3+} was recognized in two distinct fluorescence changes: one resulting from a reversible Hg^{2+}/sensor complex formation, the other an irreversible Au^{3+}-mediated hydrolysis reaction. This novel molecular structure displayed the ability to recognize both metal species at nanomolar levels.

Acknowledgements

We thank İzmir Institute of Technology (İZTECH) and TÜBİTAK for financial support.

Notes and references

1 For recent reviews, see: (*a*) M. E. Jun, B. Roy and K. H. Ahn, *Chem. Commun.*, 2011, **47**, 7583–7601; (*b*) H. Zheng, X.-Q. Zhan, Q.-N. Bian and X.-J. Zhang, *Chem. Commun.*, 2013, **49**, 429–447; (*c*) X. Chen, T. Pradhan, F. Wang, J. S. Kim and J. Yoon, *Chem. Rev.*, 2012, **112**, 1910–1956; (*d*) K. P. Carter, A. M. Young and A. E. Palmer, *Chem. Rev.*, 2014, **114**, 4564–4601; (*e*) X. Li, X. Gao, W. Shi and H. Ma, *Chem. Rev.*, 2014, **114**, 590–659.

2 (*a*) L. Xue, Q. Liu and H. Jiang, *Org. Lett.*, 2009, **11**, 3454–3457; (*b*) V. Luxami, Renukamal, K. Paul and S. Kumar, *RSC Adv.*, 2013, **3**, 9189–9192; (*c*) H. Komatsu, T. Miki, D. Citterio, T. Kubota, Y. Shindo, Y. Kitamura, K. Oka and K. Suzuki, *J. Am. Chem. Soc.*, 2005, **127**, 10798–10799; (*d*) M. Yuan, W. Zhou, X. Liu, M. Zhu, J. Li, X. Yin, H. Zheng, Z. Zuo, C. Ouyang, H. Liu, Y. Li and D. Zhu, *J. Org. Chem.*, 2008, **73**, 5008–5014; (*e*) D. Maity and T. Govindaraju, *Chem. Commun.*, 2012, **48**, 1039–1041; (*f*) P. N. Basa and A. G. Sykes, *J. Org. Chem.*, 2012, **77**, 8428–8434; (*g*) L. Cao, J. Cia, Y. Huang, Q. Zhang, N. Wang, Y. Xue and D. Du, *Tetrahedron Lett.*, 2014, **55**, 4062–4066; (*h*) N. R. Chereddy, P. Nagaraju, M. V. Niladri Raju, K. Saranraj, S. Thennarasu and V. J. Rao, *Dyes Pigm.*, 2015, **112**, 201–209; (*i*) L. Fan, J.-C. Qin, T.-R. Li, B.-D. Wang and Z.-Y. Yang, *Sens. Actuators, B*, 2014, **203**, 550–556.

3 I. Onyido, A. R. Norris and E. Buncel, *Chem. Rev.*, 2004, **104**, 5911–5929.

4 E. Nyarko, T. Hara, D. J. Grab, A. Habib, Y. Kim, O. Nikolskaia, T. Fukuma and M. Tabata, *Chem.-Biol. Interact.*, 2004, **148**, 19–25.

5 (*a*) Y.-K. Yang, K.-J. Yook and J. Tae, *J. Am. Chem. Soc.*, 2005, **127**, 16760–16761; (*b*) J.-S. Wu, I.-C. Hwang, K. S. Kim and J. S. Kim, *Org. Lett.*, 2007, **9**, 907–910; (*c*) G.-Q. Shang, X. Gao, M.-X. Chen, H. Zheng and J.-G. Xu, *J. Fluoresc.*, 2008, **18**, 1187–1192; (*d*) S. Atilgan, T. Ozdemir and E. U. Akkaya, *Org. Lett.*, 2010, **12**, 4792–4795; (*e*) Q. Zhang, X.-J. Huang and Z.-J. Zhu, *RSC Adv.*, 2013, **3**, 24891–24895; (*f*) S. Chen, P. Wang, C. Jia, Q. Lin and W. Yuan, *Spectrochim. Acta, Part A*, 2014, **133**, 223–228; (*g*) H. N. Kim, S.-W. Nam, K. M. K. Swamy, Y. Jin, X. Chen, Y. Kim, S.-J. Kim, S. Park and J. Yoon, *Analyst*, 2011, **136**, 1339–1343.

6 (*a*) M. Dong, Y.-W. Wang and Y. Peng, *Org. Lett.*, 2010, **12**, 5310–5313; (*b*) E. Karakuş, M. Üçüncü and M. Emrullahoğlu, *Chem. Commun.*, 2014, **50**, 1119–1121.

7 (*a*) M. J. Jou, X. Chen, K. M. K. Swamy, H. N. Kim, H.-J. Kim, S. G. Lee and J. Yoon, *Chem. Commun.*, 2009, 7218–7220; (*b*) O. A. Egorova, H. Seo, A. Chatterjee and K. H. Ahn, *Org. Lett.*, 2010, **12**, 401–403; (*c*) Y. K. Yang, S. Lee and J. Tae, *Org. Lett.*, 2009, **11**, 5610–5613; (*d*) J. Y. Choi, G.-H. Kim, Z. Guo, H. Y. Lee, K. M. K. Swamy, J. Pai, S. Shin, I. Shin and J. Yoon, *Biosens. Bioelectron.*, 2013, **49**, 438–441; (*e*) J.-B. Wang, Q.-Q. Wu, Y.-Z. Min, Y.-Z. Liu and Q.-H. Song, *Chem. Commun.*, 2012, **48**, 744–746; (*f*) M. Üçüncü and M. Emrullahoğlu, *Chem. Commun.*, 2014, **50**, 5884–5886; (*g*) H. Seo, M. E. Jun, O. A. Egorova, K. H. Lee, K. T. Kim and K. H. Ahn, *Org. Lett.*, 2012, **14**, 5062–5065; (*h*) M. Emrullahoğlu, E. Karakuş and M. Üçüncü, *Analyst*, 2013, **138**, 3638–3641; (*i*) S. Singha, D. Kim, H. Seo, S. W. Cho and K. H. Ahn, *Chem. Soc. Rev.*, 2015, DOI: 10.1039/c4cs00328d.

8 For recent reviews, see: (*a*) M. J. Culzoni, A. Muñoz de la Peña, A. Machuca, H. C. Goicoechea and R. Babiano, *Anal. Methods*, 2013, **5**, 30–49; (*b*) Z. Yan, M.-F. Yuen, L. Hu, P. Sun and C.-S. Lee, *RSC Adv.*, 2014, **4**, 48373–48388; (*c*) P. Mahato, S. Saha, P. Das, H. Agarwalla and A. Das, *RSC Adv.*, 2014, **4**, 36140–36174.

9 For recent reviews, see: (*a*) N. Boens, V. Leen and W. Dehaen, *Chem. Soc. Rev.*, 2012, **41**, 1130–1172; (*b*) R. Ziessel, G. Ulrich and A. Harriman, *New J. Chem.*, 2007, **31**, 496–501; (*c*) A. Loudet and K. Burgess, *Chem. Rev.*, 2007, **107**, 4891–4932; (*d*) G. Ulrich, R. Ziessel and A. Harriman, *Angew. Chem., Int. Ed.*, 2008, **47**, 1184–1201.

10 See the ESI† for more details.

11 (*a*) H. A. Benesi and J. H. Hildebrand, *J. Am. Chem. Soc.*, 1949, **71**, 2703–2707; (*b*) J. Hatai, S. Pal, G. P. Jose, T. Sengupta and S. Bandyopadhyay, *RSC Adv.*, 2012, **2**, 7033–7036.